Transactions of the Institute of Measurement and Control 29, 1 (2007) pp. 53–69

Low-dimensional model-based boundary control of 2D heat flow utilizing root locus

Mehmet Önder Efe

TOBB Economics and Technology University, Department of Electrical and Electronics Engineering, Sogutozu Cad No 43, Ankara, Turkey

Control of systems governed by Partial Differential Equations (PDEs) is an interesting subject area, as the classical tools of control theory are not directly applicable and PDEs can display enormously rich behaviour spatiotemporally. This paper considers the boundary control of a 2D heat flow problem. A solution to the control problem is obtained after a suitable model reduction. The considered PDE system is subject to Dirichlet boundary conditions of generic type $f(x)\gamma(t)$. The separation of these boundary excitations after Proper Orthogonal Decomposition yields an autonomous Ordinary Differential Equation (ODE) set in which the boundary excitations are implicit. The main contribution of this paper is to describe a mathematical treatment based on the numerical observations such that the implicit excitation terms explicitly appear in the ODE set. With such an ODE model, standard tools of feedback control theory can be applied. A measurement point has been chosen, and the desired behaviour is forced to emerge at the chosen point. A root locus technique is used to obtain the controller. It is seen that the results obtained are in good compliance with the theoretical claims.

Key words: boundary control; heat flow; model reduction; root locus.

1. Introduction

Modelling and control of Partial Differential Equation governed processes is an interesting research area, the outcomes of which address many physical phenomena

Address for correspondence: Mehmet Önder Efe, TOBB Economics and Technology University, Department of Electrical and Electronics Engineering, Sogutozu Cad No 43, Ankara, Turkey. E-mail: onderefe@ieee.org

 10.1177/0142331207073487

displaying spatial continuity, eg, heat and fluid flows. It is a well known fact that for linear Partial Differential Equations (PDEs), there are well established alternatives other than Proper Orthogonal Decomposition (POD) (Gügercin and Antoulas, 2000), but POD is a widely used method in modelling of more complicated systems. The goal of this paper is to present a bottom-up design with a discussion on the effect of parameters entering into the POD algorithm.

POD was proposed in the pioneering work of Lumley (1967) with the goal of unfolding the modal nature of turbulent flows. Sirovich (1987) introduced the method of snapshots for reducing the computational intensity of the original POD algorithm. The POD method is widely accepted as a powerful tool for decomposing the content of a time-varying spatially continuous process into the spatial and temporal components. The spatial part is a set of basis functions, whereas the temporal part is a set of differential equations. The decomposition is accomplished in the order of dominance, which is a significant property enabling the designer to truncate the expression at a particular mode number. Modelling of flow problems governed by PDEs have therefore enjoyed the POD method in obtaining the finite-dimensional models at the cost of giving concessions from the model performance, eg, Caraballo *et al*. (2004), Ly and Tran (2001), Rowley (2005), Rowley *et al*. (2004) and the references therein.

Procedurally, the PDE set is solved for the given initial and boundary conditions. Several samples from the solution set are selected and the POD method with Galerkin projection is applied. As a result of this, a set of autonomous Ordinary Differential Equations (ODEs) is obtained. The solution of the obtained ODEs with the given initial conditions synthesize the temporal part of the solution and the spatial basis functions obtained through the POD method yield the approximate solution of the PDE. Unfortunately, the set of ODEs are specific to the initial and boundary conditions used in the model derivation stage. In other words, one needs to change the ODE model for every different instance of boundary excitation regimes and this is a significant problem for the boundary control goal. This paper demonstrates how the aforementioned autonomous set of ODEs is made non-autonomous and external excitations are seen explicitly in the model. Aside from making the boundary excitations explicit in the model, the validity of the developed model is extended to a set of boundary conditions, which constitute the final stage of the modelling effort. The prominent feature of the approach presented here is that the algorithm yields a model using some boundary excitations, but the model maintains its validity for different but similar signals. The modelling procedure was followed with pointwise boundary excitations for 1D Burgers equation in Efe and Özbay (2004) and 2D heat equation in Efe and Özbay (2003). This paper extends the boundary excitations to non-point subdomains of the boundaries, which results in much richer heat distributions in the snapshots than those obtained in Efe and Özbay (2003).

Another variation of the low-dimensional (LD) modelling of a 2D heat flow problem has been taken into consideration by Atwell and King (2001), who consider a modified 2D heat transport problem with control input explicitly available in the PDE. The thermal diffusivity parameter has been taken as a known constant and several control strategies have been assessed with the modelling results of the POD approach. Clearly, the availability of the control input in the PDE means that the excitation is not only

through the boundaries, and the obtained low-order model would have the excitations explicitly.

Once the finite-dimensional model for an infinite-dimensional process is obtained, one might base the design on the LD model and implement a boundary controller for the original process. Optimal control is one of the frequently used approaches in boundary control applications of PDE systems. One work focusing on a 1D heat conduction problem reported the design of time-optimal boundary control (Mizel and Seidman, 1997), with the emphasis that the time-optimal control has the bang-bang property, and the solution has been postulated by the techniques of Hilbert spaces. Rösch (1994) viewed the characterization of boundary condition as an identification problem, and presented an iterative approach to meet the conditions of optimality. Ravindran (2000) and Singh *et al*. (2001) followed the optimal control techniques on more complicated flow systems, namely a flow past a step (Ravindran, 2000) and flow past a cylinder (Singh *et al*., 2001). Both of these works dealt with Navier–Stokes equations.

This paper is organized as follows. The second section summarizes the POD algorithm specific to the modelling of a 2D heat flow problem. In the third section, development of the reduced-order model for the 2D heat flow is analysed. The fourth section presents the modelling results with an emphasis on the spectral dependence of the model on the operating conditions. In the fifth section, the design and analysis of the observer is presented and the feedback control design is explained in the sixth section. The seventh section summarizes the contribution of the paper to the subject area and positions the paper within the cited references with emphasis on the introduced originality. The concluding remarks are given at the end of the paper.

2. Proper orthogonal decomposition

Consider the ensemble $U_i(x,y)$, $i = 1,2,\ldots N_s$, where N_s is the number of elements. Every element of this set corresponds to a snapshot observed from a process, eg, 2D heat flow with initial and boundary conditions,

$$\begin{aligned} u_t(x,y,t) &= c^2(u_{xx}(x,y,t) + u_{yy}(x,y,t)) \\ u(x,0,t) &= f_1(x)\gamma_1(t) \\ u(1,y,t) &= f_2(y)\gamma_2(t) \\ u(x,1,t) &= f_3(x)\gamma_3(t) \\ u(0,y,t) &= f_4(y)\gamma_4(t) \\ u(x,y,0) &= 0 \quad \forall (x,y) \end{aligned} \tag{1}$$

where c is the known constant thermal diffusivity parameter, and the subscripts x, y and t refer to the partial differentiation with respect to x, y and time, respectively. The continuous time process takes place over the physical domain $\Omega := \{(x,y) \mid (x,y) \in [0,1] \times [0,1]\}$ and the solution is obtained on a spatial grid denoted by Ω_d, which describes the co-ordinates of the pixels of every snapshot in the ensemble. The entities described over Ω_d are matrices in $\Re^{Ny \times Nx}$. Note that in (1), $f_i(\cdot)$ for each i is a function that describes how $\gamma_i(t)$ influences the behaviour along the corresponding edge of Ω.

$f_i(\cdot)$s can be selected arbitrarily, yet for every i, $f_i(0) = f_i(1) = 0$, so that the problem description is consistent at the corners of Ω, and $\gamma_i(t)$ becomes independent from $\gamma_j(t)$ for $i \neq j$ and the external excitations can be selected arbitrarily.

With this problem description, the goal of applying POD is to find an orthonormal basis set letting us write the solution as

$$u(x,y,t) = \sum_{i=1}^{R_L} \alpha_i(t)\Phi_i(x,y) \tag{2}$$

where $\alpha_i(t)$ is the ith temporal mode, $\Phi_i(x,y)$ is the ith spatial function (basis function or the eigenfunction), R_L is the number of independent basis functions that can be synthesized from the given ensemble, or equivalently that spans the space described by the ensemble. It will later be clear that if the basis set $\{\Phi_i(x,y)\}_{i=1}^{R_L}$ is an orthonormal set, Galerkin projection yields the autonomous set of ODEs directly. Let us summarize the POD procedure.

Step 1. Calculate the $N_s \times N_s$ dimensional correlation matrix L, the ijth entry of which is $L_{ij} = \langle U_i, U_j \rangle_{\Omega_d}$, where $\langle \cdot, \cdot \rangle_{\Omega_d}$ is the inner product operator defined over $\Re^{\mathrm{Ny} \times \mathrm{Nx}}$.

Step 2. Find the eigenvectors (denoted by v_i) and the associated eigenvalues (λ_i) of the matrix L. Sort them in a descending order in terms of the magnitudes of λ_i. Note that every v_i is an $N_s \times 1$ dimensional vector satisfying $v_i^T v_i = 1/\lambda_i$, here, for simplicity of the exposition, it is assumed that the eigenvalues are distinct.

Step 3. Construct the basis set by using

$$\Phi_i(x,y) = \sum_{j=1}^{N_s} v_{ij} U_j(x,y) \tag{3}$$

where v_{ij} is the jth entry of the eigenvector $v_i = (v_{i1} \quad v_{i2} \quad \ldots \quad v_{iN_s})^T$, and $i = 1,2, \ldots, R_L$, with $R_L = \mathrm{rank}(L)$. It can be shown that $\langle \Phi_i(x,y), \Phi_j(x,y) \rangle_\Omega = \delta_{ij}$ with δ_{ij} being the Kronecker delta function. Notice that the basis functions are admixtures of the snapshots (Efe and Özbay, 2003; Ly and Tran, 2001).

Step 4. Calculate the temporal coefficients. Taking the inner product of both sides of (2) with $\Phi_i(x,y)$, the orthonormality property leads to

$$\begin{aligned} \alpha_i(t_0) &= \langle \Phi_i(x,y), u(x,y,t_0) \rangle_\Omega \\ &= \langle \phi_i, U_{t_0} \rangle_{\Omega_d} \\ &:= \frac{1}{N_s} \sum_{l=1}^{N_x} \sum_{j=1}^{N_y} \phi_i(x_l, y_j) U_{t_0}(x_l, y_j) \\ &:= \phi_i(x,y) * U_{t_0}(x,y) \end{aligned} \tag{4}$$

where $\phi_i \in \Re^{\mathrm{Ny} \times \mathrm{Nx}}$ is a sampled form of the basis function Φ_i defined over Ω. The operator denoted by * computes a real number that is the sum of all elements of a matrix obtained through the elementwise multiplication of the two matrices that * lies in between. Without loss of generality, an element of the ensemble $\{U_i(x,y)\}_{i=1}^{N_s}$ may be $U(x,y,t_0)$. Therefore, in order to generate the temporal gain, $\alpha_k(t)$, of the spatial

eigenfunction ϕ_k, one would take the inner product of ϕ_k with the elements of the ensemble as given below,

$$\begin{aligned} \langle U_1, \phi_k \rangle_{\Omega_d} &\approx \alpha_k(t_1) \\ \langle U_2, \phi_k \rangle_{\Omega_d} &\approx \alpha_k(t_2) \\ &\vdots \\ \langle U_{N_s}, \phi_k \rangle_{\Omega_d} &\approx \alpha_k(t_{N_s}) \end{aligned} \tag{5}$$

The above computation is important for making a comparison between the quantities obtained from the decomposition [see (5)] and the quantities obtained from the model. Note that the temporal coefficients satisfy orthogonality properties over the discrete set $t \in \{t_1, t_2, \ldots, t_{Ns}\}$ [see (6)].

$$\sum_{i=1}^{N_s} \langle U_i(x,y), \Phi_k(x,y) \rangle_{\Omega_d}^2 \approx \sum_{i=1}^{N_s} \alpha_k^2(t_i) = \lambda_k \tag{6}$$

For a more detailed discussion on the POD method, the reader is referred to Caraballo *et al*. (2004), Efe and Özbay (2003–2004), Lumley (1967), Ly and Tran (2001), Rowley (2005), Rowley *et al*. (2004), and the references therein.

Fundamental assumption: The majority of works dealing with POD and model reduction applications presume that the flow is dominated by coherent modes, which means that the flow can be decomposed into distinguishable components in the order of dominance. Because of the dominance of coherent modes, the typical spread of the eigenvalues of the correlation matrix turns out to be logarithmic and the terms decay very rapidly in magnitude. This fact enables us to assume that a reduced-order representation, say with M modes ($M < R_L$), can also be written as an equality

$$u(x,y,t) = \sum_{i=1}^{M} \alpha_i(t) \Phi_i(x,y) \tag{7}$$

and the reduced-order model is derived under the assumption that (7) satisfies the governing PDE in (1) (Caraballo *et al*., 2004; Efe and Özbay, 2003, 2004; Ly and Tran, 2001; Ravindran, 2000). Unsurprisingly, such an assumption results in a model having uncertainties; however, one should keep in mind that the goal is to find a model, which matches the infinite-dimensional system in some sense of approximation with typically $M > R_L < N_s$. To represent how good such an expansion is, a percentage energy measure is defined as follows

$$E = 100 \frac{\sum_{i=1}^{M} \lambda_i}{\sum_{i=1}^{R_L} \lambda_i} \tag{8}$$

where the tendency of $E \to 100\%$ means that the model captures the dynamical information contained in the snapshots well. Conversely, an insufficient model will be obtained if E is far below 100%. Clearly, POD lets us reduce the dimensionality of the problem from infinity to R_L, and the fundamental assumption further enables us to reduce the LD model order to M. In the next section, how the boundary conditions are

transformed into explicit control terms in the corresponding set of ODEs is demonstrated.

3. Reduced-order modelling

In the order reduction phase, we need to obtain the autonomous ODE model first. Towards this goal, if (7) is a solution to the PDE in (1), then it has to satisfy the PDE. Substituting (2) into (1) with the fundamental assumption yields

$$\sum_{i=1}^{M} \dot{\alpha}_i(t)\Phi_i(x,y) = c^2 \sum_{i=1}^{M} \alpha_i(t)\Psi_i(x,y) \tag{9}$$

where $\Psi_i(x,y) = \Phi_{i\ xx}(x,y) + \Phi_{i\ yy}(x,y)$. Taking the inner product of both sides with $\Phi_k(x,y)$ and remembering $\langle \Phi_i(x,y)\Phi_k(x,y)\rangle_\Omega = \delta_{ik}$, with δ_{ik} being the Kronecker delta, results in

$$\dot{\alpha}_k(t) = c^2 \sum_{i=1}^{M} \alpha_i(t)\langle \Phi_k(x,y), \Psi_i(x,y)\rangle_\Omega \tag{10}$$

Defining ζ_k as the entity in Ω_d corresponding to the entity Ψ_k in Ω, one could rewrite (10) as

$$\dot{\alpha}_k(t) = c^2 \sum_{i=1}^{M} \alpha_i(t)\langle \phi_k, \zeta_i\rangle_{\Omega_d} \tag{11}$$

Equation (11) can be written explicitly by using * operator as

$$\dot{\alpha}_k(t) = c^2 \sum_{i=1}^{M} \alpha_i(t)(\phi_k(x,y)*\zeta_i(x,y)) \tag{12}$$

Notice that * operator can be applied individually over $\Omega_d^1, \Omega_d^2, ..., \Omega_d^n$, which are n non-overlapping subdomains of Ω_d such that $\Omega_d^1 \cup \Omega_d^2 \cup ... \cup \Omega_d^n = \Omega_d$. This lets us separate the entries corresponding to boundaries without modifying the value of $\langle \phi_k, \zeta_i\rangle_{\Omega_d}$, ie, $\phi_k(x,y)*\zeta_i(x,y)$ as seen in (13),

$$\begin{aligned}\dot{\alpha}_k(t) = {} & c^2 \sum_{i=1}^{M} \alpha_i(t)(\phi_k(x,0)*\zeta_i(x,0) + \phi_k(1,y)*\zeta_i(1,y) + \phi_k(x,1)*\zeta_i(x,1) + \phi_k(0,y)*\zeta_i(0,y)) \\ & + c^2 \sum_{i=1}^{M} \alpha_i(t)(\phi_k^o(x,y)*\zeta_i^o(x,y))\end{aligned} \tag{13}$$

In the above, $\phi_k^o(x,y)$ denotes a matrix that is obtained when the boundary elements of $\phi_k(x,y)$ are removed, ie, the first and the last rows, and columns. Similarly, in the computation of terms like $\phi_k(x,0)*\zeta_i(x,0)$, the terms $\phi_k(x,0)$ and $\zeta_i(x,0)$ correspond to the first rows of the matrices $\phi_k(x,y)$ and $\zeta_i(x,y)$, respectively.

The kth component of the first summation in (13), which is obtained when $i = k$, can be separated from the expression and (14) is obtained, which lets us embed the boundary conditions into the expression,

$$\dot{\alpha}_k(t) = c^2\alpha_k(t)(\phi_k(x,0)*\zeta_k(x,0) + \phi_k(1,y)*\zeta_k(1,y) + \phi_k(x,1)*\zeta_k(x,1) + \phi_k(0,y)*\zeta_k(0,y))$$

$$+c^2\sum_{i=1}^{M}\alpha_i(t)(1-\delta_{ik})(\phi_k(x,0)*\zeta_i(x,0) + \phi_k(1,y)*\zeta_i(1,y) + \phi_k(x,1)*\zeta_i(x,1)$$

$$+\phi_k(0,y)*\zeta_i(0,y)) + c^2\sum_{i=1}^{M}\alpha_i(t)(\phi_k^o(x,y)*\zeta_i^o(x,y)) \tag{14}$$

At this stage of the modelling, we need to paraphrase the boundary conditions in such a way that the final expression above can be incorporated with these conditions. The underlying idea is straightforward: if (7) is a solution, then it must be satisfied at the boundaries as well, ie,

$$\sum_{i=1}^{M}\alpha_i(t)\phi_i(x,0) = f_1(x)\gamma_1(t) \tag{15}$$

which can be paraphrased as

$$\alpha_k(t)\phi_k(x,0) = f_1(x)\gamma_1(t) - \sum_{i=1}^{M}(1-\delta_{ik})\alpha_i(t)\phi_i(x,0) \tag{16}$$

Similarly,

$$\sum_{i=1}^{M}\alpha_i(t)\phi_i(1,y) = f_2(y)\gamma_2(t) \tag{17}$$

which can be rewritten as

$$\alpha_k(t)\phi_k(1,y) = f_2(y)\gamma_2(t) - \sum_{i=1}^{M}(1-\delta_{ik})\alpha_i(t)\phi_i(1,y) \tag{18}$$

We can perform the same arrangement for the remaining two edges as given below:

$$\sum_{i=1}^{M}\alpha_i(t)\phi_i(x,1) = f_3(x)\gamma_3(t) \tag{19}$$

$$\alpha_k(t)\phi_k(x,1) = f_3(x)\gamma_3(t) - \sum_{i=1}^{M}(1-\delta_{ik})\alpha_i(t)\phi_i(x,1) \tag{20}$$

$$\sum_{i=1}^{M} \alpha_i(t)\phi_i(0,y) = f_4(y)\gamma_4(t) \tag{21}$$

and

$$\alpha_k(t)\phi_k(0,y) = f_4(y)\gamma_4(t) - \sum_{i=1}^{M}(1-\delta_{ik})\alpha_i(t)\phi_i(0,y) \tag{22}$$

Concatenating the obtained terms in one expression yields

$$\begin{aligned}\dot{\alpha}_k(t) &= c^2(f_1(x)*\zeta_k(x,0))\gamma_1(t) + c^2(f_2(y)*\zeta_k(1,y))\gamma_2(t) + c^2(f_3(x)*\zeta_k(x,1))\gamma_3(t)\\ &+c^2(f_4(y)*\zeta_k(0,y))\gamma_4(t) + c^2\sum_{i=1}^{M}\alpha_i(t)(\phi_k*\zeta_i - \phi_i(x,0)*\zeta_k(x,0)\\ &-\phi_i(1,y)*\zeta_k(1,y) - \phi_i(x,1)*\zeta_k(x,1) - \phi_i(0,y)*\zeta_k(0,y))\end{aligned} \tag{23}$$

which can be written compactly as

$$\dot{\alpha}(t) = A\alpha(t) + B\Gamma(t) \tag{24}$$

where $\alpha(t) = (\alpha_1(t)\ \ \alpha_2(t)\ \ \ldots\ \ \alpha_M(t))^T$ is the state vector, $\Gamma(t) = (\gamma_1(t)\ \ \gamma_2(t)\ \ \gamma_3(t)\ \ \gamma_4(t))^T$ is the input vector and

$$\begin{aligned}A_{ki} &= \phi_k(x,y)*\zeta_i(x,y) - \phi_i(x,0)*\zeta_k(x,0) - \phi_i(1,y)*\zeta_k(1,y)\\ &-\phi_i(x,1)*\zeta_k(x,1) - \phi_i(0,y)*\zeta_k(0,y)\end{aligned} \tag{25}$$

and the kth row of the input matrix is

$$B_k = c^2(f_1(x)*\zeta_k(x,0)\quad f_2(y)*\zeta_k(1,y)\quad f_3(x)*\zeta_k(x,1)\quad f_4(y)*\zeta_k(0,y)) \tag{26}$$

This result practically lets us have a representative linear dynamical model for the infinite-dimensional process in (1), which is aimed to be controlled through the boundaries. The next section presents to what extent the modelling strategy discussed here could be successful.

4. Justification of the dynamic model

According to the described procedure, several tests have been done. Due to the numerical advantages, the PDE has been solved by using the Crank–Nicholson method (see Farlow, 1993, for details), with a step size of 1 ms. The initial thermal distribution is taken as zero everywhere and the thermal diffusivity constant is set as $c = 2$. In order to form the solution, a linear grid having $N_x = N_y = 25$ points in the x-direction and y-direction, respectively. According to the above parameter values, a set of 501 snapshots embodies the entire numerical solution, among which linearly sampled $N = 251$ snapshots have been used for the POD scheme. Although one may use the entire set of snapshots, it has been shown by Sirovich (1987) that a reasonably descriptive subset of them can be used for the same purpose. In the literature, this

approach is called the *method of snapshots*, which significantly reduces the computational intensity of the overall scheme (see also Ravindran, 2000, and Ly and Tran, 2001). Once the modes have been obtained, the solution at $M = 9$ is truncated, which represents 99.9704% of the total energy described in the denominator of the expression in (8).

In order to demonstrate the performance of the dynamic model, we choose the functions that are effective along the boundaries as $f_1(x) = \sin(2\pi x)$, $f_1(y) = \sin(2\pi y)$, $f_3(x) = -\sin(2\pi x)$ and $f_4(y) = -\sin(2\pi y)$ are chosen. As the temporal excitations, the following input signals are chosen,

$$\gamma_1(t) = 5\sin(2\pi 70t(T - t)) \tag{27}$$

$$\gamma_2(t) = 5\sin\left(2\pi 55t\left(\frac{T}{2} - t\right)\right) \tag{28}$$

$$\gamma_3(t) = 5\sin\left(2\pi 65t\left(\frac{T}{3} - t\right)\right) \tag{29}$$

$$\gamma_4(t) = 5\sin\left(2\pi 50t\left(\frac{T}{4} - t\right)\right) \tag{30}$$

where $T = 0.5$ s. The choice of the above excitation signals is deliberate as they are spectrally rich enough. As can be seen from Figure 1, values of $\alpha_k(t)$ will undergo regimes that change sometimes slowly and sometimes fast depending on the spectral composition of the external inputs. Under these conditions, the response of the LD model is illustrated in Figure 2, in which every subplot contains two curves. Obviously, the temporal variables obtained from the POD algorithm are very close to those obtained from the LD model and this observation indicates that the LD model is a good representative for the chosen test conditions.

Undoubtedly, one would expect a good match between the state variables obtained from the POD algorithm and the state variables obtained through the numerical solution of the ODE set in (24). One might question whether the model is specific to the boundary conditions above. Remedying this is accomplished by choosing another set of external inputs and obtaining the response of the model without modifying the model parameters. For this purpose,

$$\gamma_1(t) = \sin(2\pi 70t(0.6 - t)) \tag{31}$$

$$\gamma_2(t) = \sin\left(2\pi 55t\left(\frac{T}{4} - t\right)\right) \tag{32}$$

$$\gamma_3(t) = \sin\left(2\pi 60t\left(t - \frac{T}{3}\right)\right) \tag{33}$$

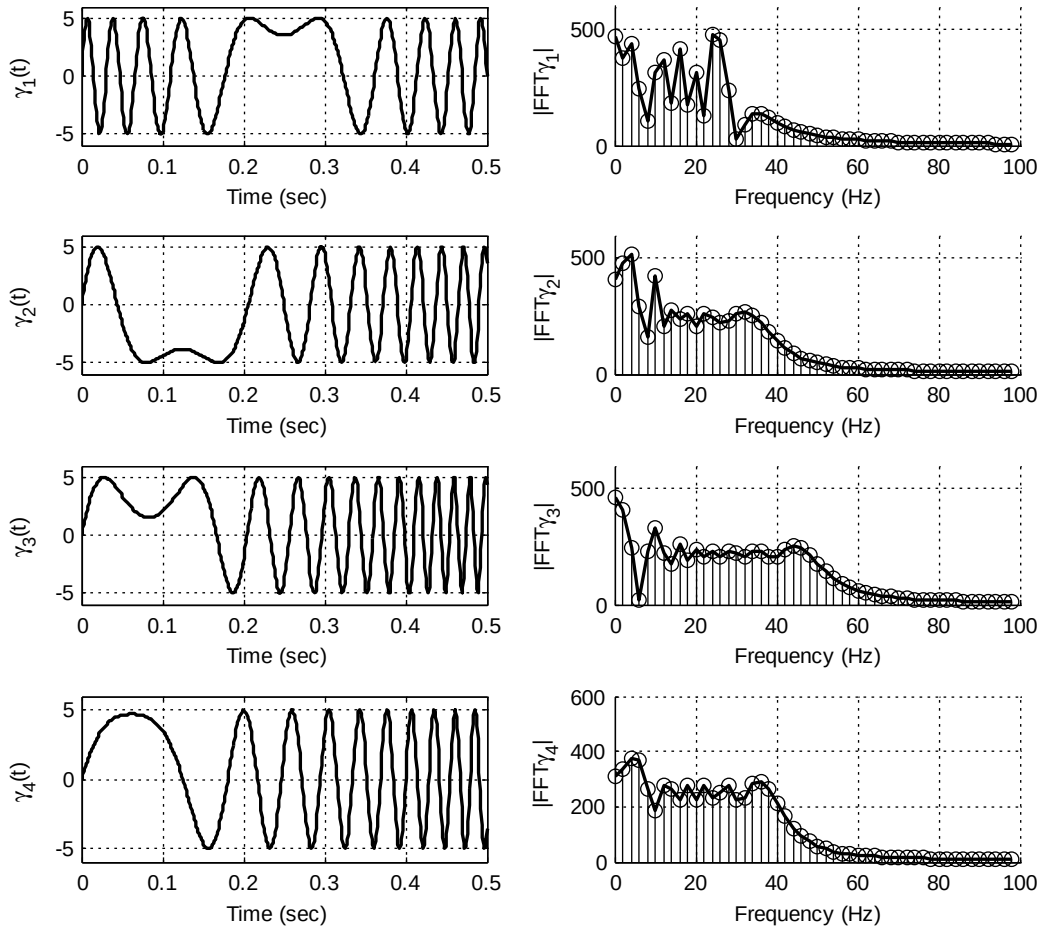

Figure 1 Temporal and spectral views of the boundary excitations used in the derivation of the low-order model

$$\gamma_4(t) = \sin\left(2\pi 45t\left(\frac{T}{5} - t\right)\right) \tag{34}$$

and the results obtained are illustrated in Figures 3 and 4. It is seen that the state variables are obtained precisely when the relevant signal changes slowly. During the regions where the signals change quickly, there is some visible discrepancy due to the spectral dependence of the model properties to the signals used during the derivation of the model, which are illustrated in the right subplots of Figure 1. To justify this claim, take the Laplace transform of the PDE in (1) and write the general solution as below:

$$s\mathrm{U}(x,y,s) - u(x,y,0) = c^2(\mathrm{U}_{xx}(x,y,s) + \mathrm{U}_{yy}(x,y,s)) \tag{35}$$

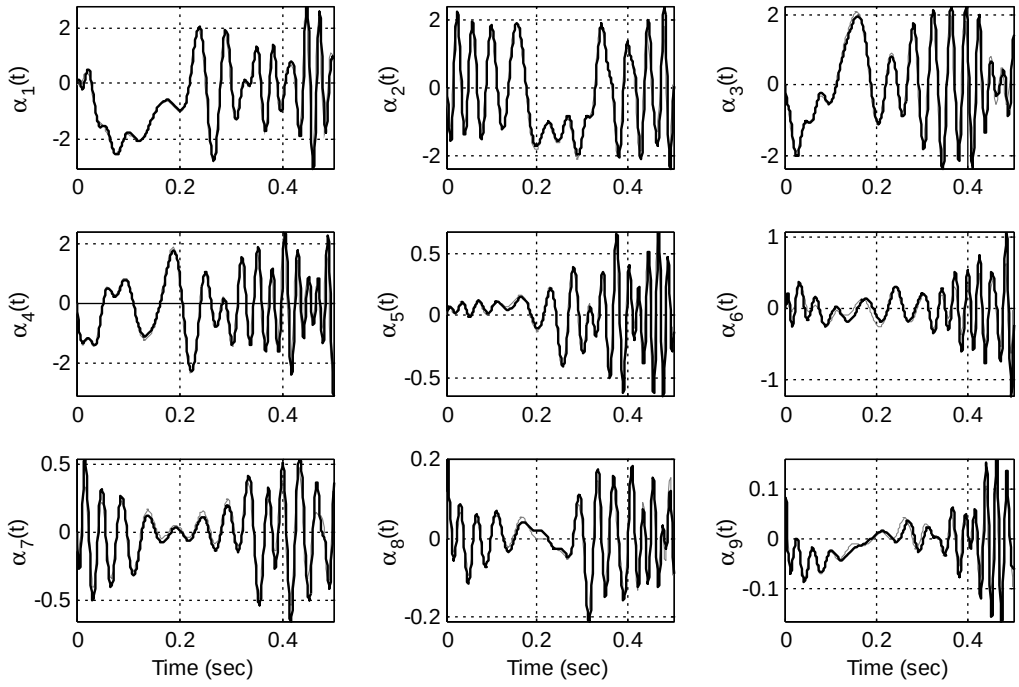

Figure 2 The state variables ($\alpha_k(t)$) obtained from POD and those from the LD model in (24)

where $u(x,y,0)$ has been specified to be zero over Ω. This would produce the following general solution

$$\mathrm{U}(x,y,s) = C_1(s)e^{x\sqrt{s}/c} + C_2(s)e^{-x\sqrt{s}/c} + C_3(s)e^{y\sqrt{s}/c} + C_4(s)e^{-y\sqrt{s}/c} \tag{36}$$

Referring to the four boundary conditions in (1) with the chosen $f_1(x)$, $f_2(y)$, $f_3(x)$ and $f_4(y)$, one can write four equalities to solve for the unknown $C_i(s)$, which are $\mathrm{U}(1/4,\ 0, s) = \Gamma_1(s)$, $\mathrm{U}(1,\ 1/4,\ s) = \Gamma_2(s)$, $\mathrm{U}(3/4,\ 1, s) = \Gamma_3(s)$ and $\mathrm{U}(0,\ 3/4,\ s) = \Gamma_4(s)$. This lets us have the following matrix equality;

$$\begin{pmatrix} C_1(s) \\ C_2(s) \\ C_3(s) \\ C_4(s) \end{pmatrix} = \begin{pmatrix} e^{\sqrt{s}/4c} & e^{-\sqrt{s}/4c} & 1 & 1 \\ e^{\sqrt{s}/c} & e^{-\sqrt{s}/c} & e^{\sqrt{s}/4c} & e^{-\sqrt{s}/4c} \\ e^{3\sqrt{s}/4c} & e^{-3\sqrt{s}/4c} & e^{\sqrt{s}/c} & e^{-\sqrt{s}/c} \\ 1 & 1 & e^{3\sqrt{s}/4c} & e^{-3\sqrt{s}/4c} \end{pmatrix}^{-1} \begin{pmatrix} \Gamma_1(s) \\ \Gamma_2(s) \\ \Gamma_3(s) \\ \Gamma_4(s) \end{pmatrix} \tag{37}$$

After the inversion,

$$\mathrm{U}(x,y,s) = \mathrm{H}_1(x,y,s)\Gamma_1(s) + \mathrm{H}_2(x,y,s)\Gamma_2(s) + \mathrm{H}_3(x,y,s)\Gamma_3(s) + \mathrm{H}_4(x,y,s)\Gamma_4(s) \tag{38}$$

Once the external excitations are specified, it becomes visible that the spectral content $\mathrm{U}(x,y,j\omega)$ is determined by the transfer functions $\mathrm{H}_i(x,y,j\omega)$ and the external excitations, $\Gamma_i(t)$. This representation clearly supports the conclusion of spectral dependence of the LD model to the signals used during the model derivation stage.

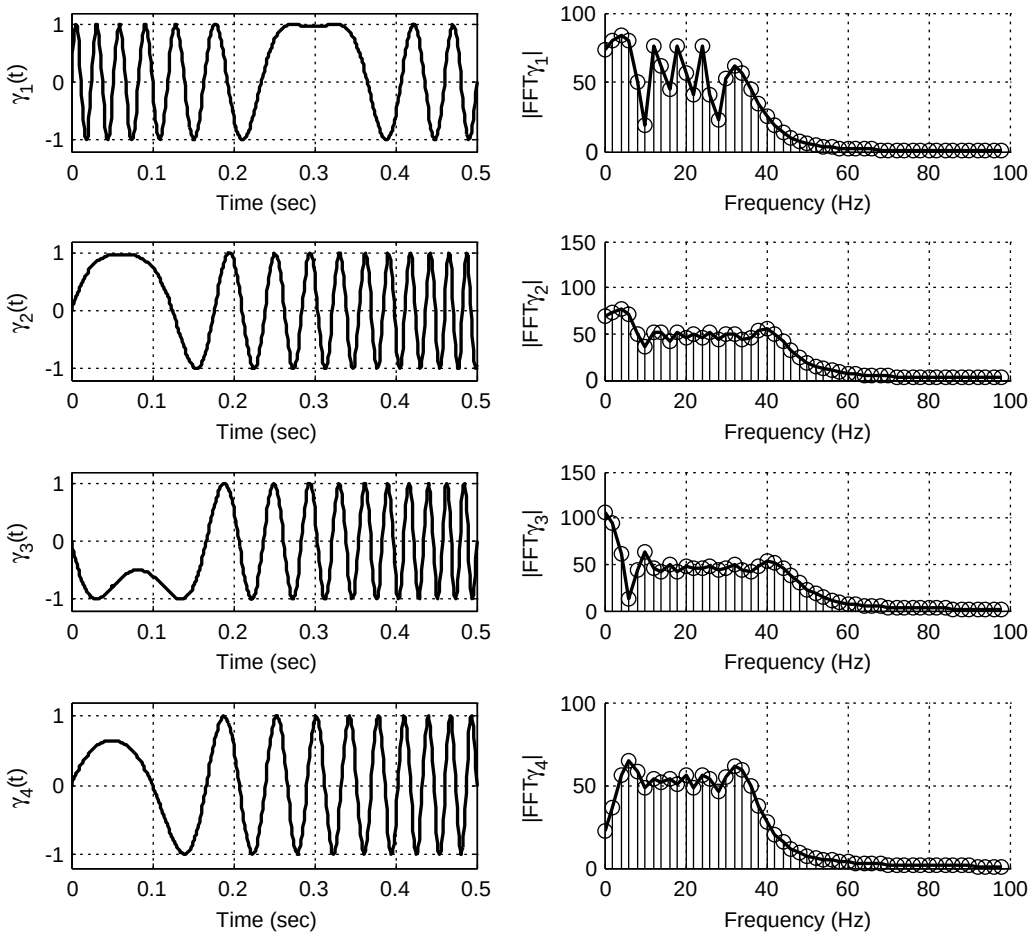

Figure 3 Temporal and spectral views of the test boundary excitations

One should keep in mind that the linearity of the PDE under investigation has facilitated achieving this conclusion. If the boundary signals are spectrally rich enough, then their effects are reflected to the snapshots [see (38)] as much as the system dynamics in (1) permits. This can also be seen from $u(x,y,t) = \Sigma_{i=1}^{4} \int_0^t \mathrm{h}_i(x,y,t-\tau)\gamma_i(\tau)\mathrm{d}\tau := U_t$ with $\mathrm{h}_i(x,y,t)$ being the inverse Laplace transform of $\mathrm{H}_i(x,y,s)$. Unsurprisingly, the properties specified indirectly by the snapshots will be inherited by the LD model. As a result, the richer the boundary excitations spectrally, the better the snapshots containing the spectral properties of the system dynamics. To sum up, the signals used in the modelling stage have significant effects on the performance of the LD model and those signals have to excite the system persistently in order to obtain a reasonably descriptive model. This is one important contribution of this paper. The next section focuses on how a root locus-based feedback controller can be designed for the PDE process in (1).

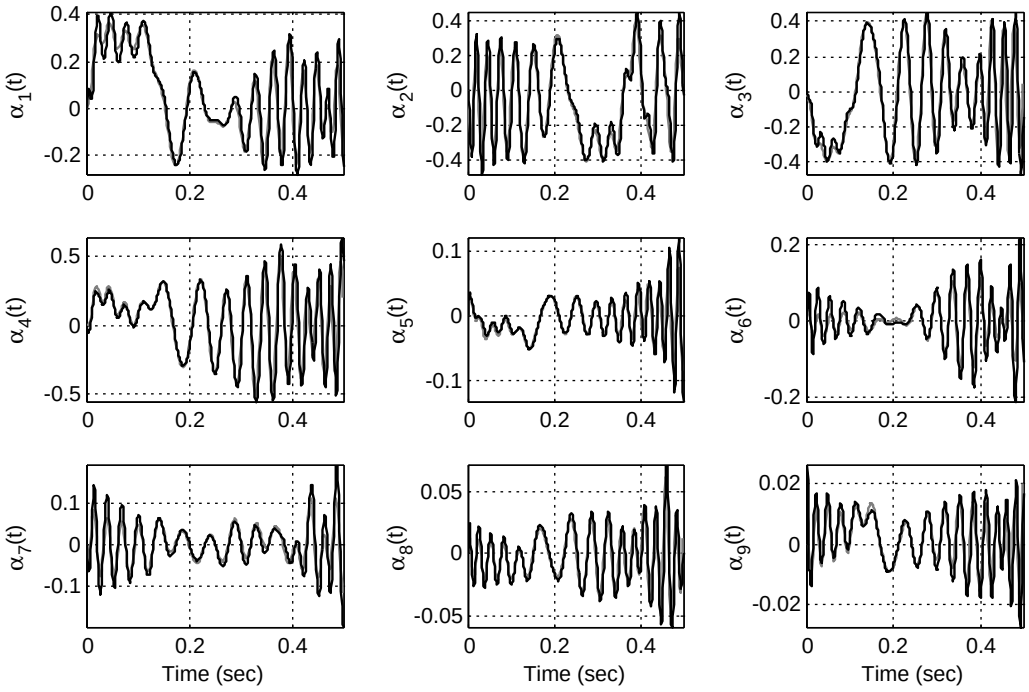

Figure 4 The state variables ($\alpha_k(t)$) obtained from POD and those from the LD model in (24) for the test boundary excitations

5. Root locus-based boundary control of 2D heat flow

Root locus is a very powerful technique in linear systems theory. As the representative model of the process is a finite-dimensional linear plant, the technique for designing a simple yet effective feedback controller can be utilized. In this paper, the following scenario is studied. As illustrated in Figure 5, the inputs γ_2, γ_3 and γ_4 are the entries of external disturbances while γ_1 is reserved for the control signal. The matrix B is partitioned as $B = (B_c \quad B_d)$, where B_c is $M \times 1$ vector and B_d is an $M \times 3$ matrix.

The control problem is to force the behaviour at a measurement point towards a desired profile by altering $\gamma_1(t)$ appropriately. The process output, $u(x,y,t)$, is

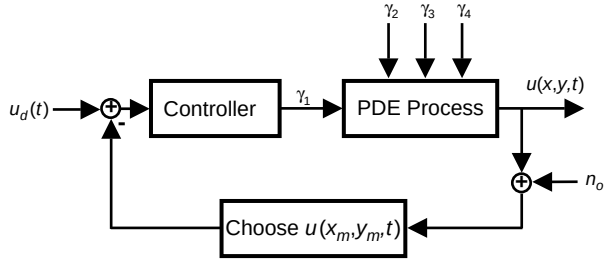

Figure 5 Block diagram of the feedback control system

corrupted by a spatially continuous noise signal, $n_o(x,y,t)$, whose power is 0.002 and $u(x,y,0)$ is randomly set. The other disturbance signals are $\gamma_2(t) = 0.1\sin(40\pi t)$, $\gamma_3(t) = 0.1\,\text{sign}(\sin(50\pi t))$ and $\gamma_4(t) = 0.1\sin(90\pi t)$. Such disturbance entries excite the PDE process both abruptly and smoothly, thereby letting us see the disturbance rejection capability of the closed-loop control system. As the reference signal,

$$r(t) = \begin{cases} \sin(4\pi t) & 0 \le t \le 1 \text{ s} \\ \text{sign}(\sin(4\pi t)) & 1 \le t \le 3 \text{ s} \end{cases} \tag{39}$$

is chosen, which lets us see the performance under smooth and sharp command signals. To achieve the goal, notice first that the open-loop system is Type 0 and introduce a pole at $s = 0$ to make the open-loop transfer function Type I. Although this is sufficient to track very slowly changing command signals for the problem at hand, a real pole at $s = -1000$ is further added to modify the root locus, so that the closed-loop poles may be placed more comfortably so that rise time is reduced significantly. Utilizing the graphical tools of Matlab®, the gain of the controller is adjusted so that no overshoot in the step response is observed. The global and zoomed root locus plots taking the poles introduced by the controller into account are illustrated in Figure 6, from which one can see the locations of the closed-loop poles too.

According to the above discussion and the design efforts, the controller is given as

$$C(s) = 200\frac{1}{s(1 + 0.001s)} \tag{40}$$

The results of the simulations are shown in Figure 7, where the top subplot depicts the command signal and the measurement from the PDE process, $u(x_m,y_m,t)$ with $x_m = 5\Delta x$ and $y_m = 5\Delta y$, where $\Delta x = 1/(N_x - 1)$ and $\Delta y = 1/(N_y - 1)$. The process output closely follows the reference signal and this observation enables us to conclude with the usefulness of the POD-based LD model. The middle subplot of Figure 7 shows the difference $r(t) - u(x_m,y_m,t)$. The trend seen emphasizes that the error is suppressed successfully by the controller. The bottom subplot of the figure shows the applied control signal, $\gamma_1(t)$. The control signal is reasonably smooth and the controller is successful in rejecting the disturbances admissibly, which are two prominent features of the controller.

The results justify the following claim: the design of a feedback boundary controller can be based upon a reduced-order model that can be obtained through the POD algorithm. The next section summarizes the contributions of the paper to the subject area.

6. Contributions and conclusions

This paper considers POD-based LD modelling of 2D heat flow and its control through boundaries. The paper validates the model and emphasizes that the model is useful over a set of operating conditions. The boundary control is achieved by a simple controller obtained through the use of the root locus technique. The simulation results have met the expectations and the following major and minor contributions have been made.

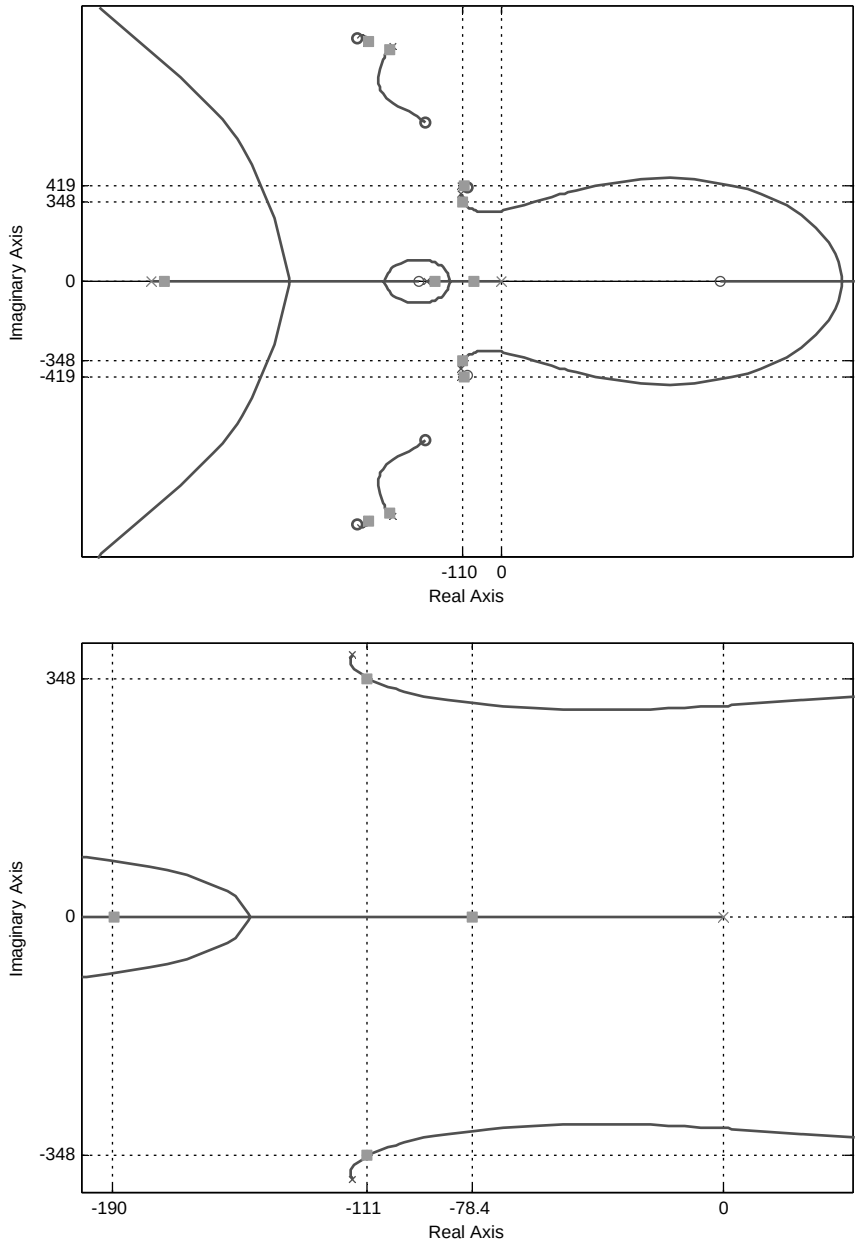

Figure 6 Root locus plots with the contribution of the controller: (a) global view (top); (b) near origin view (bottom)

The paper demonstrates a bottom-up procedure letting us use a very standard tool of control theory for the control of processes governed by PDEs. This is the major focus and the key contribution of the paper. Another major contribution of the paper is the demonstration of the spectral dependence of the LD model on the operating

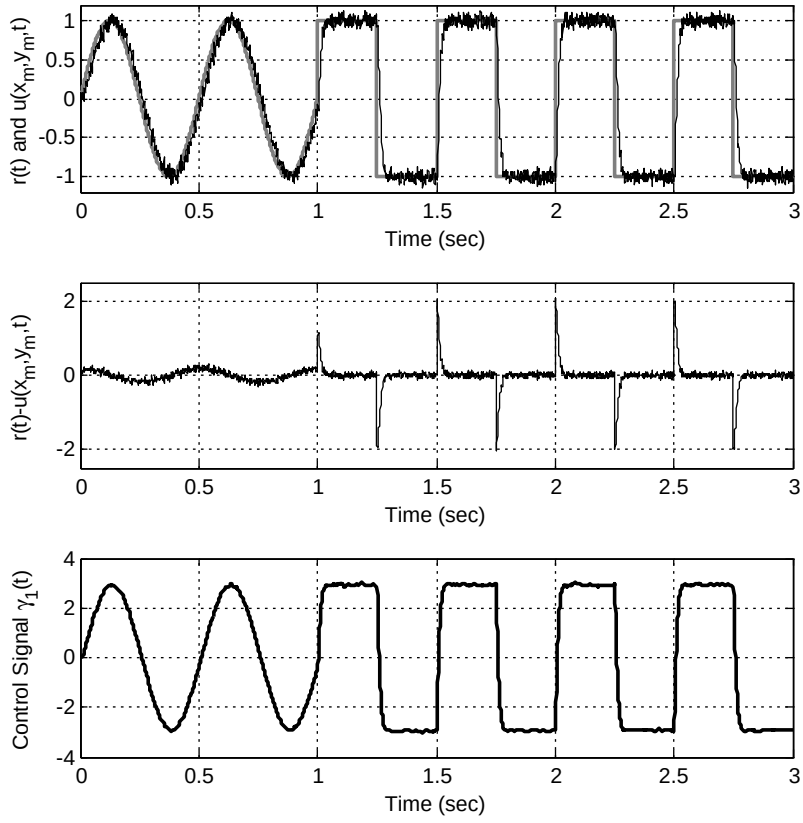

Figure 7 Simulation results

conditions in the model derivation stage. The paper shows that the choice of the external excitations is substantially important in terms of the LD model performance and this has a guiding nature in the implementation of POD, as a very high level of captured energy does not imply a satisfactory performance by itself.

The last major contribution is the assessment of the importance of the fundamental assumption. The bottom-up design is strongly based on to what extent this assumption holds true. As the number of modes in the model increases, more energy is captured and a better approximation is obtained. Consequently, the confidence in the design on the fundamental assumption is increased and the model uncertainty becomes negligible, yet the model starts losing its usefulness in the increasing direction of M, which is a significant parameter in modelling studies exploiting the POD approach. This discussion demonstrates how critical the hold of the fundamental assumption is.

Aside from the major results above, one of the minor contributions is the extension of a previously proposed approach from pointwise excitation to excitations along non-point subdomains, ie, the excitation along the boundaries. The separation scheme lets us use the model not only for predetermined boundary control regimes (Efe, 2003, 2004), but also for a set of boundary excitations. The second minor contribution is better understanding of POD, which is achieved by choosing a linear system.

Needless to say, the linearity of the PDE has been exploited in drawing the above conclusions. These conclusions, and the modelling and control strategy investigated in this paper, advance the subject area to the clarification of the following fact: POD is a powerful technique but its usefulness depends upon the PDE in hand, problem settings and the associated operating conditions.

Acknowledgements

This work is supported by TOBB ETU BAP Program (Contract No: ETU BAP 2006/04). The author would like to thank Prof. Hitay Özbay, Prof. Mo Samimy, Dr James H. Myatt, Dr J. DeBonis, Dr Marco Debiasi, Dr Russell C. Camphouse, Dr Peng Yan, Xin Yuan and Edgar Caraballo for fruitful discussions in devising the presented work.

References

Atwell, J.A. and **King, B.B.** 2001: Proper orthogonal decomposition for reduced basis feedback controllers for parabolic equations. *Mathematical and Computer Modelling of Dynamical Systems* 33, 1–19.

Caraballo, E., Malone, J., Samimy, M. and **DeBonis, J.** 2004: A study of subsonic cavity flows: low dimensional modeling. *AIAA Paper*, 2004–124.

Efe, M.Ö. and **Özbay, H.** 2003: Proper orthogonal decomposition for reduced order modeling: 2D heat flow. *Proceedings of the IEEE International Conference on Control Applications (CCA'2003)*, Istanbul, Turkey, 23–25 June, 1273–78.

Efe, M.Ö. and **Özbay, H.** 2004: Low dimensional modeling and Dirichlet boundary controller design for Burgers equation. *International Journal of Control* 77, 895–906.

Farlow, S.J. 1993: *Partial differential equations for scientists and engineers*. Dover Publications Inc., 317–22.

Gügercin, S. and **Antoulas, A.C.** 2000: A comparative study of 7 model reduction algorithms. *Proceedings of the 39th IEEE Conference on Decision and Control*, Sydney.

Lumley, J. 1967: The structure of inhomogeneous turbulent flows. *Atmospheric Turbulence and Wave Propagation*. Nauca, 166–76.

Ly, H.V. and **Tran, H.T.** 2001: Modeling and control of physical processes using proper orthogonal decomposition. *Mathematical and Computer Modelling of Dynamical Systems* 33, 223–36.

Mizel, V.J. and **Seidman T.I.** 1997: An abstract bang-bang principle and time-optimal boundary control of the heat equation. *SIAM Journal on Control and Optimization* 35, 1204–16.

Ravindran, S.S. 2000: A reduced order approach for optimal control of fluids using proper orthogonal decomposition. *International Journal for Numerical Methods in Fluids* 34, 425–88.

Rösch, A. 1994: Identification of nonlinear heat transfer laws by optimal control. *Numerical Functional Analysis and Optimization* 15, 417–34.

Rowley, C.W. 2005: Model reduction for fluids, using balanced proper orthogonal decomposition. *International Journal of Bifurcation and Chaos* 15, 997–1013.

Rowley, C.W., Colonius, T. and **Murray, R.M**. 2004: Model reduction for compressible flows using POD and Galerkin projection. *Physica D-Nonlinear Phenomena* 189, 115–29.

Singh, S.N., Myatt, J.H., Addington, G.A., Banda, S. and **Hall, J.K.** 2001: Optimal feedback control of vortex shedding using proper orthogonal decomposition models. *Transactions of the ASME: Journal of Fluids Engineering* 123, 612–18.

Sirovich, L. 1987: Turbulence and the dynamics of coherent structures. *Quarterly of Applied Mathematics* XLV, 561–90.